Published online 4 September 2009

Nucleic Acids Research, 2009, Vol. 37, No. 20 ***e137***
doi:10.1093/nar/gkp715

A high throughput experimental approach to identify miRNA targets in human cells

Lu Ping Tan[1], Erwin Seinen[2], Gerben Duns[3], Debora de Jong[1], Ody C. M. Sibon[2], Sibrand Poppema[1], Bart-Jan Kroesen[4], Klaas Kok[3] and Anke van den Berg[1,*]

[1]Department of Pathology and Laboratory Medicine, [2]Department of Cell Biology/Radiation and Stress Cell Biology, [3]Department of Genetics and [4]Department of Medical Biology, University Medical Center Groningen, University of Groningen, Hanzeplein 1, 9700 RB Groningen, The Netherlands

Received May 18, 2009; Revised July 16, 2009; Accepted August 14, 2009

ABSTRACT

The study of human microRNAs is seriously hampered by the lack of proper tools allowing genome-wide identification of miRNA targets. We performed Ribonucleoprotein ImmunoPrecipitation—gene Chip (RIP-Chip) using antibodies against wild-type human Ago2 in untreated Hodgkin lymphoma (HL) cell lines. Ten to thirty percent of the gene transcripts from the genome were enriched in the Ago2-IP fraction of untreated cells, representing the HL miRNA-targetome. *In silico* analysis indicated that ~40% of these gene transcripts represent targets of the abundantly co-expressed miRNAs. To identify targets of miR-17/20/93/106, RIP-Chip with anti-miR-17/20/93/106 treated cells was performed and 1189 gene transcripts were identified. These genes were analyzed for miR-17/20/93/106 target sites in the 5′-UTRs, coding regions and 3′-UTRs. Fifty-one percent of them had miR-17/20/93/106 target sites in the 3′-UTR while 19% of them were predicted miR-17/20/93/106 targets by TargetScan. Luciferase reporter assay confirmed targeting of miR-17/20/93/106 to the 3′-UTRs of 8 out of 10 genes. In conclusion, we report a method which can establish the miRNA-targetome in untreated human cells and identify miRNA specific targets in a high throughput manner. This approach is applicable to identify miRNA targets in any human tissue sample or purified cell population in an unbiased and physiologically relevant manner.

INTRODUCTION

MicroRNAs (miRNAs) are small RNAs of 19–23 nucleotides which were first discovered less than two decades ago in *Caenorhabditis elegans* (1). Upon binding to Argonaute (Ago) proteins, the RNA induced silencing complex (RISC) is formed for post-transcriptional silencing of genes (2). It is now known that numerous cellular processes including proliferation, differentiation, apoptosis and cell cycle are under regulatory control of miRNAs (3).

Expression of miRNAs can be highly tissue specific (4) and dynamic, as for example seen in hematopoiesis (5,6). The cell physiological impact of miRNA expression was shown by skewing of hematopoeitic stem cell differentiation towards a specific hematopoeitic cell type by changing the expression level of only one miRNA (7). Due to the powerful influence of miRNAs as master regulators of gene expression, it is evident that abnormal expression of miRNAs may contribute to malignant transformation.

Accurate target gene validation has been proven notoriously difficult as apparent by the relatively few miRNA targets that have been experimentally proven thus far. Taken into account that 10–30% of the genes from the genome are predicted to be under the control of miRNAs (8,9), many miRNA:mRNA interactions are still unknown. Several algorithms are available to predict miRNA target genes (8,10,11). However, the consistency between different miRNA prediction algorithms available is limited and the false positive rate is high (8,12). Results from the prediction programs require experimental validation, such as by luciferase reporter assay and western blotting. Current genome wide screenings approaches include microarray analyses, two-dimensional fluorescence Difference Gel Electrophoresis (2D-DIGE) and

*To whom correspondence should be addressed. Tel: +31 50 3611476; Fax: +31 50 3619107; Email: a.van.den.berg@path.umcg.nl

The authors wish it to be known that, in their opinion, the second and third authors should be regarded as joint Second Authors.

stable isotope labeling with amino acids in culture (SILAC) (13,14). However, each of these approaches have their specific caveats including lack of effect at the mRNA level, labor intensiveness, accuracy, complexity of the proteome and protein half life.

Recently, several studies reported application of an interesting new biochemical approach to analyze cellular mRNA associated with RISC (15–20). In human cells the immunoprecipitation (IP) of Ago protein was combined with overexpression of synthetic miRNAs (18–20). Moreover, flag-tagged Ago proteins were used requiring a significant modulation of the cells which may result in target genes that are not physiologically relevant. The lack of high throughput methods to accurately identify miRNA targets relevant to a specific cell type in an unbiased manner hampers the progression in the discovery of miRNA targets.

In this study, we describe an approach which allows large scale identification of miRNA targets in untreated cells. In this adapted Ribonucleoprotein ImmunoPrecipitation—gene Chip (RIP-Chip) approach, wild-type human Ago2 protein is directly immunoprecipitated from untreated cells. The Ago2-associated mRNA transcripts are analyzed by microarray to identify the miRNA-targetome (whole miRNA regulated gene set) of a specific cell. Moreover, by combining this approach with inhibition of specific miRNAs, we established an approach which allows large-scale identification of endogenous transcripts that are targeted by a specific miRNA. This strategy provides unbiased identification of physiologically relevant miRNA target genes.

MATERIALS AND METHODS

Cell culture and transfection

The HL cell lines, L428 and L1236 were cultured in RPMI 1640 supplemented with ultraglutamine, 100 U/ml penicillin/streptomycin, and 5 or 10% fetal bovine serum (Cambrex Biosciences, Walkersville, USA), respectively. Cells were diluted 1 : 2 on the day prior to transfection and/or Ago2 immunoprecipitation.

Locked nucleic acid (LNA) with phosphorothioate (PS) backbone antisense to miR-17-5p, miR-20a, miR-93, miR-106a and miR-106b (Integrated DNA Technologies, Leuven, Belgium) were pooled to form a cocktail of anti-miR-17/20/93/106. LNA antisense to miR-220 was used as a negative control as miR-220 is not expressed in L428 (21). Transfection of cell lines was performed using the Amaxa nucleofector I device (Amaxa, Gaithersburg, USA) with solution L, program X-01 for L428 and solution V, program T-01 for L1236. For the RIP-Chip experiment, 5-million cells were transfected with 2.5 nmol of anti-miR-17/20/93/106 or anti-miR-220 and the cells were harvested 16 h later. Effective silencing of miR-17/20/93/106 in the cell lines (L428 and L1236) had been proven with luciferase reporter assay and western blot for *CDKN1A*/p21 (data not shown), a proven miR-17 seed family target (22).

RIP-Chip: IP and western blotting

IP of ribonucleoprotein was performed as previously described (23) in both HL cell lines (L1236 and L428) with and without transfection of anti-miR-17/20/93/106 and additionally L428 with transfection of anti-miR-220 as a negative control. Briefly, 10–20-million cells were lysed in 100 µl ice cold polysome lysis buffer (5 mM $MgCl_2$, 100 mM KCl, 10 mM Hepes, pH7.0 and 0.5% Nonidet P-40) with freshly added 1 mM DTT, 100 U/ml Rnase OUT (Invitrogen, Carlsbad, USA) and 1× complete mini EDTA free protease inhibitor cocktail (Roche, Basel, Switzerland) for 5 min. Centrifugation was carried out two times at 14 000*g* at 4°C for 10 min. Supernatant was mixed with 900 µl of ice-cold NT2 buffer (50 mM Tris, pH 7.4, 150 mM NaCl, 1 mM $MgCl_2$, 0.05% Nonidet P-40) containing freshly added 200 U/ml Rnase OUT (Invitrogen, Carlsbad, USA), 0.5% vanadyl ribonucleoside (Invitrogen, Carlsbad, USA), 1 mM DTT, 15 mM EDTA and 50 µl mouse anti-human Ago2 (Clone 2E12-1C9, Abnova, Taipei City, Taiwan) coated sepharose G beads (Abcam, Cambridge, UK). Incubation was carried out overnight at 4°C on a rocking platform. On the following day, beads were washed five times with ice-cold NT2 buffer and separated into two portions—one for RNA isolation to identify miRNA target genes and another portion for western blotting to check for successful IP of Ago2. Mouse IgG_1 isotype control (Abcam, Cambridge, UK) was used as a negative control for the IP procedure. The mouse anti-Ago2 used in the IP was also used for western blotting at a dilution of 1 : 1000 while secondary antibody was rabbit anti mouse conjugated with horse radish peroxidase (Dako, Glostrup, Denmark), also at a dilution of 1 : 1000. For visualization, the blot was incubated 5 min with SuperSignal West Pico Chemiluminescent Substrate (ThermoScientific, Rockford, USA) prior to exposure to film.

RIP-Chip: RNA isolation and microarray analysis

RNA from the flow through (FT) fraction of untransfected L1236, total cell lysate fractions and Ago2-IP fractions of all cells were isolated using Trizol and glycogen (all from Invitrogen, Carlsbad, USA) as a carrier in the ethanol precipitation step. RNA quality was checked with the 2100 Bioanalyzer (Agilent, Santa Clara, USA) and the concentration was determined by Nanodrop 1000 (Thermo Scientific, Wilmington, USA). Microarray analysis was performed according to the manufacturer's protocol (Agilent, Santa Clara, USA). Briefly, first strand cDNA was synthesized from 200 ng RNA, followed by cRNA amplification and labeling with Cy3 or Cy5. Purification of Cy3 or Cy5 labeled cRNA was carried out with Qiagen RNeasy Mini kit (Qiagen, Venlo, Netherlands). The cRNA quantity and labeling specificity were determined using the NanoDrop 1000 (Thermo Scientific, Wilmington, USA). Equal amounts of Cy3 or Cy5 labeled cRNA from the Ago2-IP or FT fraction and from the corresponding total cell lysate fraction were mixed and hybridized in a dye swap design at 65°C overnight on Agilent 44k 60-mer Human Whole Genome Oligo Microarray. On the following day, slides

were washed and signals were scanned with GenePix 4000B (Agilent, Santa Clara, USA). Signal intensities from scanned images were processed and converted into Linear and Lowess normalized data using Agilent Feature Extraction software version 9.1. Quality control report was generated for each array. Using GeneSpring GX version 9.0 (Agilent, Santa Clara, USA), the abundance of probes in the Ago2-IP or FT fraction was compared with the abundance in the total fraction. For each probe, the signal intensity from the Ago2-IP or FT RNA fraction was divided by the signal intensity from the total cell lysate RNA fraction (IP/*T* or FT/*T*). For each dye swap, the average IP/*T* or FT/*T* ratio was calculated. Any gene transcript corresponding to a probe with an average IP/*T* ratio of at least 2 was considered as being enriched in the Ago2-IP fraction, representing the miRNA-targetome (Table 1 and Supplementary Data 1). IP/*T* of each probe from the untransfected cells was compared with IP/*T* of those in the cells transfected with antisense oligonucleotides (Supplementary Data 1). Two criteria were set to identify miR-17 seed family specific miRNA targets: (i) the probes must be present in the Ago2-IP fraction (IP/*T*>2) of untransfected cells and (ii) in the transfected cells, the probes should show ≥2-fold depletion from the Ago2-IP fraction when compared with the Ago2-IP fraction of untransfected cells. Different depletion folds from the Ago2-IP fraction upon specific miRNA inhibition were used to generate probe sets for seed matching site analysis and prediction by algorithms. The data described in this publication have been deposited in NCBI's Gene Expression Omnibus (24) and are accessible through GEO Series accession number GSE14409 (http://www.ncbi.nlm.nih.gov/geo/query/acc.cgi?acc=GSE14409).

In silico analysis of miRNA seed matching sites

For the HL miRNA-targetome, 3′-UTRs of all gene transcripts were analyzed for 8-mer site matching to the top 5% most abundant miRNAs in L428 and L1236 (23 out of 470 miRNAs assessed, representing 10 miRNA seed families (21), Supplementary Data 2). MiR-155 was excluded from the search because it was highly expressed in L1236 but only moderately (not top 5%) in L428. To identify targets of the miR-17 seed family, 6-mer and 8-mer sites in the 3′-UTRs were analyzed. The 6-mer site is considered as the least stringent requirement for miRNA targeting while an 8-mer site is considered to be the most reliable indication for miRNA targeting (14). Additionally, conditions like 5′-UTRs, coding sequences and GU wobble were included in the analysis for miR-17 seed family targeting. Since any short sequence has a very high occurrence throughout the genome, the miRNA seed matching sites were first subjected to a background analysis to calculate the percentage of gene transcripts in the genome with the exact site matches within all known 3′-UTR sequences of all human genes. The 3′-UTR sequences were downloaded from the UCSC website (release March 2006) and loaded into a MySQL database server for convenience using our own programmed importing tool (available upon request). Using specific queries we could identify any miRNA seed matching site and its occurrence throughout the genome. Probe sets generated from the RIP-Chip experiment were analyzed with this method and compared with the results obtained from the genome. All information about miRNA seed matching sites for each probe in the miRNA-targetome can be found in Supplementary Data 1.

miRNA target prediction

TargetScan release 5.0 was used to predict targets of the 10 miRNA seed familes and miBridge was used to predict miR-17 seed family targets (11,25). For TargetScan, only conserved miRNAs that target conserved gene transcripts were considered. Not all gene transcripts identified in the RIP-Chip experiment were included in the database of the prediction programs because most of the time only the Refseq transcripts or only one of the 3′-UTR for any gene, rather than all 3′-UTRs of all transcripts, are included.

Luciferase reporter assay

3′-UTRs of 13 genes (Table 2) were cloned into psiCHECK2 vector for luciferase reporter assay (Promega, Madison, USA) as previously described (21). L428 was chosen for luciferase reporter assay because L428 showed higher cell viability and transfection efficiency as compared with L1236. Briefly, the sequence of interest (Supplementary Data 3) was cloned behind the renilla luciferase (RL) gene in the psiCHECK2 vector. The insert was checked by sequencing. The firefly luciferase (FL) gene present in the same vector was used for normalization to rule out variation in transfection efficiency across samples. One to two-million L428 cells transfected with 2 μg of each construct with or without 2 nmol of anti-miR-17/20/93/106 were harvested 48 h post transfection for dual luciferase measurement. RL/FL ratio of cells transfected only with the construct was set at 100%. Changes in RL/FL ratio in cells cotransfected with anti-miR-17/20/93/106 are shown as percentage compared with the control. All transfections were repeated at least three times to demonstrate consistency of the results and calculate standard deviations.

RESULTS

RIP-Chip of untreated HL cells

Protein coding mRNA transcripts which serve as target genes for miRNAs are bound indirectly to the Ago-containing RISC (Figure 1A). An antibody against wild-type human Ago2 was used to immunoprecipitate the RISC from the total cell lysate of HL cell lines L1236 and L428. IP was validated by western blotting, showing Ago2 protein in the total cell lysate and the Ago2-IP fraction, while the Ago2 protein was absent in the flow through (FT) fraction. A mouse isotype control (IgG1) antibody was used as a negative control. Here, western blot showed Ago2 protein in the total cell lysate and in

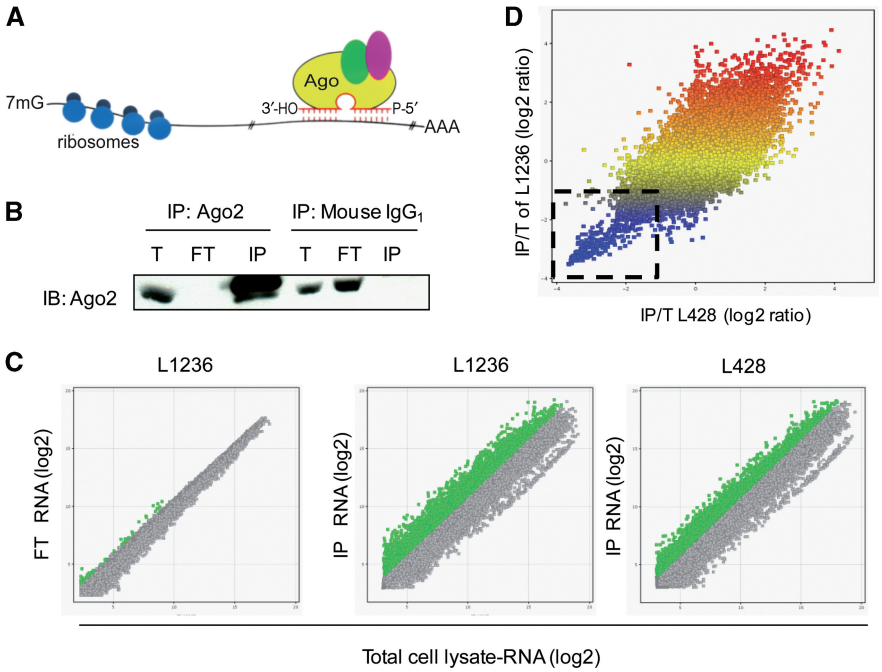

Figure 1. RIP-Chip for identification of Ago2 associated gene transcripts. (**A**) Schematic diagram of the RNA induced silencing complex (RISC) mediated gene silencing. (**B**) IP of Ago2 complex, analyzed by western blotting (IB). Ago2 was pulled down when appropriate antibody was used. Mouse IgG1 was used as a negative control and indeed revealed no IP of Ago2. (**C**) Microarray analysis showed that 43 probes in flow through (FT) of L1236, 3164 probes in IP of L1236 and 2703 probes in IP of L428 (highlighted in green) were more than 2-fold enriched compared with the total cell lysate (T). (**D**) Probe sets enriched in the Ago2-IP showed a good correlation in both Hodgkin lymphoma cell lines. Probes representing the 'non-miRNA targets' (IP/T<0.5) were outlined in open box with dash line.

Table 1. Numbers of probes enriched in FT or Ago2-IP fraction as compared with total cell lysate

	FT/T	IP/T	
	L1236	L1236	L428
>4	1	882	398
>2	43	3164	2703
>1	15 075	12 409	15 178

FT, flow through fraction. T, total cell lysate. IP, immunoprecipitated fraction.

the FT, but not in the IP fraction (Figure 1B). Using gene expression arrays, the signal intensities of probes associated with Ago2-IP were compared with the signal intensities of probes in the total cell lysate fraction (IP/T ratio). Different IP/T thresholds (1, 2 and 4) were applied to determine the probes enriched in the IP fraction. A threshold of IP/T>1 resulted in the identification of 12 409 probes in L1236 and 15 178 probes in L428 enriched in the Ago2-IP fractions. An IP/T>2 reduced the number of probes enriched in the IP fraction to 3164 in L1236 and 2703 in L428 (Figure 1C and Table 1). With a threshold of IP/T>4, the number of probes enriched in the IP fraction was reduced to 882 in L1236 and 398 in L428. As an additional control, we also analyzed the FT of L1236 in the same way, this revealed 15 075, 43 and 1 probe using an FT/T threshold of 1, 2 and 4, respectively. Based on the results observed in FT/T, and considering the fact that 10–30% of the genes from the genome are predicted to be under the control of miRNAs (8,9), we chose IP/T>2 as the threshold for miRNA target genes and collectively called all gene transcripts in this category as the HL miRNA-targetome. Interestingly, the miRNA-targetome of L1236 and L428 shared a marked overlap but also showed distinct differences (Figure 1D). These differences are caused by minor discrepancies in transcriptome and differences in the extent of miRNA regulation between L1236 and L428.

In silico analysis of the HL miRNA-targetome

Three thousand one hundred sixty-four probes (representing 2746 unique gene transcripts and 2629 genes) in L1236 and 2703 probes (representing 2431 unique gene transcripts and 2363 genes) in L428 with IP/T>2 were considered as the miRNA-targetome of the corresponding cell lines and these probe sets were studied to assess miRNA targeting *in silico*. The probe set with IP/T<0.5 in both untreated HL cell lines (Figure 1D) was termed as 'non-miRNA targets' and used as a negative control. The top 5% expressed miRNAs in L428 and L1236 (21) harbored 10 different seed sequences (Supplementary Data 2). These miRNAs were considered to be the miRNA candidates accountable for a main part of the miRNA-targetome. Two aspects were used as definitions for miRNA targets: (i) presence of miRNA 8-mer seed matching site in the 3′-UTR and (ii) prediction by TargetScan release 5.0. All information about miRNA

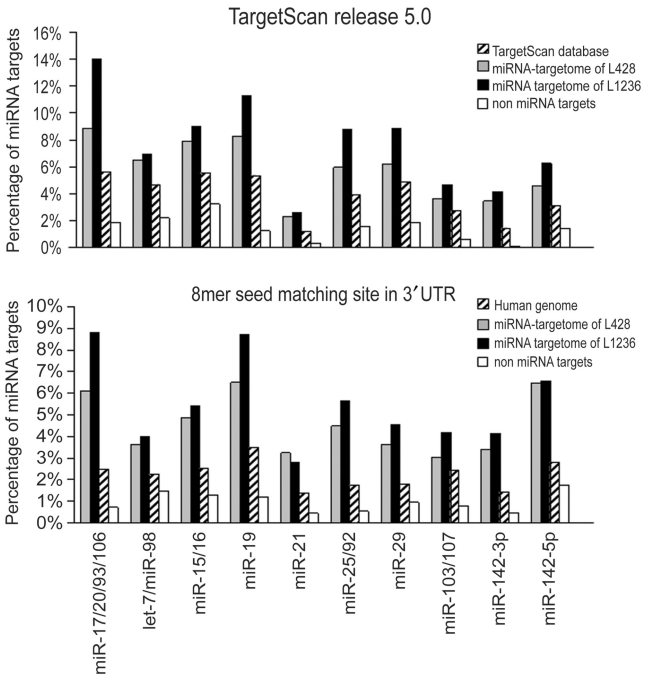

Figure 2. Enrichment of miRNA targets is apparent in miRNA-targetome of HL but not in 'non-miRNA targets'. Definitions of miRNA targets were (i) prediction of targeting by TargetScan release 5.0 and (ii) presence of 8-mer site in the 3′-UTRs. In both definitions the percentage of miRNA targets was always higher in the miRNA-targetome of HL (L428 and L1236) and lowest in the 'non-miRNA targets', when compared with genome or the whole database.

seed matching sites and TargetScan prediction for each probe in the miRNA-targetome can be found in Supplementary Data 1.

In the analysis of 3′-UTRs for 8-mer site matching to each of the 10 seeds of the top 5% expressed miRNAs, the percentage of miRNA targets was always higher in the miRNA-targetome of both cell lines as compared with the genome (Figure 2). Moreover, about 32% of the miRNA-targetome of both HL cell lines contained the 8-mer sites of at least one of the 10 seeds whereas this was only 18% in the genome. Notably, 10% of the miRNA-targetome of both HL cell lines contained at least two 8-mer sites of the top 5% expressed miRNAs.

According to the TargetScan release 5.0, the miRNA-targetome of both HL cell lines contained higher percentages of miRNA targets of the 10 seed families when compared with the percentage in the database (Figure 2). About 30 and 40% of the miRNA-targetome of L1236 and L428, respectively, were predicted as targets of at least one of the top 5% expressed miRNAs whereas only 24% of all genes present in the TargetScan database were predicted targets of at least one of the top 5% expressed miRNAs. The percentage of genes predicted to be targeted by at least two of the top 5% expressed miRNAs was 9% for all genes in the TargetScan database, 15 and 21% in the miRNA-targetome of L428 and L1236, respectively.

In contrast to the enrichment of miRNA targets observed in the HL miRNA-targetome, the percentage of miRNA targets in 'non-miRNA targets' was always lower compared with the genome (Figure 2).

Our data indicated that we obtained a significant enrichment of miRNA targets in the Ago2-IP fraction (i.e. miRNA-targetome). In HL, the top 5% expressed miRNAs could already be sufficient to regulate up to ~40% of the miRNA-targetome. The remaining 60% of the miRNA-targetome is assumed to be regulated by other miRNAs which are moderately expressed in HL.

Anti-miRNA strategy combined with RIP-Chip

As miRNAs from the miR-17 seed family comprised a large proportion of the top 5% expressed miRNAs in HL (21) and are frequently associated with the regulation of cell cycle, we proceed with anti-miRNA strategy combined with RIP-Chip to identify the endogenous miR-17 seed family targets in HL.

Upon inhibition of miRNAs of the miR-17 seed family by antisense oligonucleotides, targets of the miR-17 seed family are depleted from the Ago2-IP fraction and remain in the FT fraction (Figure 3A). In order to identify targets of the miR-17 seed family in a high throughput manner, RIP-Chip was carried out in both HL cell lines (L1236 and L428) with transfection of anti-miR-17/20/93/106, and the data were compared with the data of untransfected cells. Validation of the IP procedure by western blots revealed a positive staining of Ago2 in the total and the Ago2-IP fraction whereas no Ago2 was observed in the FT fraction (Figure 3B). This showed that the IP procedure was successful. RNA was isolated from the total and Ago2-IP fraction of all cells and were subjected to microarray analysis. By comparing IP/T values of untransfected and anti-miR-17/20/93/106 transfected cells, 493 probes in L428 and 895 probes in L1236 were $\geq$2-fold depleted from the Ago2-IP fraction as compared with untransfected cells (highlighted in blue, Figure 3C). Probes with <2-fold depletion were considered as 'not depleted'. In addition to the $\geq$2-fold depletion, we also analyzed the probe sets showing $\geq$3–7-fold depletion for targeting by the miR-17 seed family (Supplementary Data 4). The 'not depleted' probes in L428 and L1236 were merged together as the 'non-miR-17 targets', probe sets with $\geq$2 depletion fold in both cell lines as the 'miR-17 targets', and probe sets with $\geq$4-fold depletion in L428 and $\geq$7-fold depletion in L1236 as the 'potent miR-17 targets' (gene transcripts with highest depletion fold). Every gene transcript isoform was considered as a unique entity and this led to 3163 'non-miR-17 targets', 1189 'miR-17 targets' and 66 'potent miR-17 targets'. As a control, we also compared the IP/T values of untransfected and anti-miR-220 transfected L428 cells, which revealed only 211 probes that were $\geq$2-fold depleted from the Ago2-IP fraction (highlighted in blue, Figure 3C).

Analysis of miR-17 binding sites for miR-17 targets identified in RIP-Chip

Every gene transcript from the human genome was inspected for the presence of miR-17 seed matching sites (6-mer and 8-mer) in the 3′-UTR and analyzed with prediction programs (miBridge and TargetScan). In all

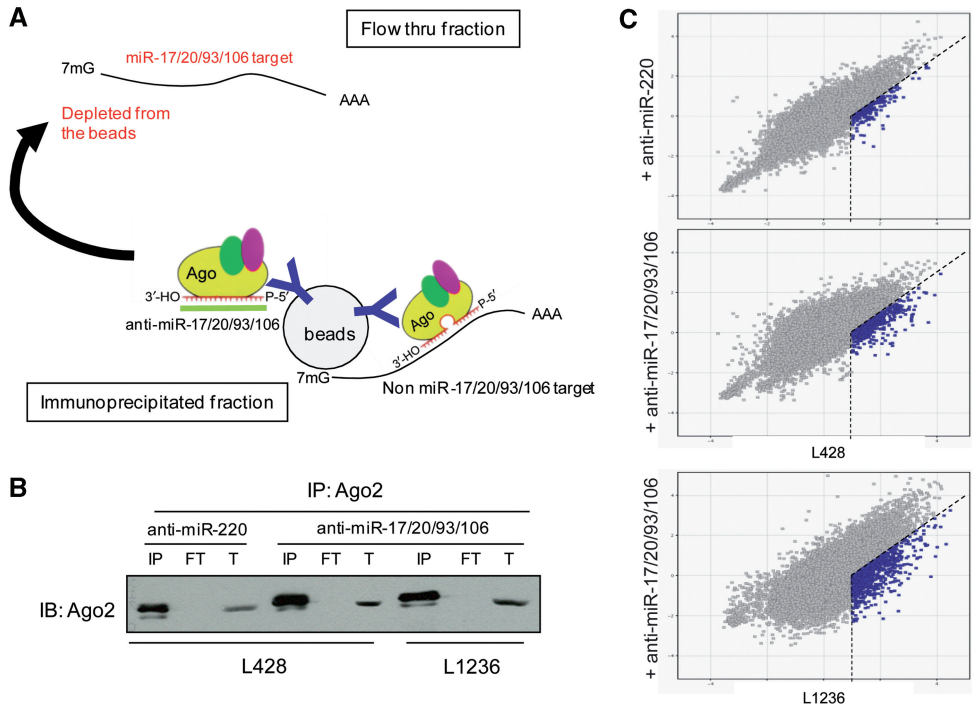

Figure 3. Identification of targets of the miR-17 seed family. (**A**) Schematic diagram of targets of the miR-17 seed family depleted from the RISC upon miR-17/20/93/106 inhibition. The letter Y represents antibody directed against Ago2 and black thin lines with 7mG in front and AAA in the end represent mRNAs. (**B**) IP of Ago2 complex from anti-miR-17/20/93/106 and anti-miR-220 transfected cells, analyzed by western blotting (IB). (**C**) RIP-Chip: expression profiles of Ago2-IP RNA from anti-miR-220 and miR-17/20/93/106 transfected cells were compared with the untransfected cells. Probes which were present in the untransfected Ago2-IP fraction (IP/T>2) and ≥2-fold depleted from the Ago2-IP fraction upon miRNA inhibition were outlined with dash line.

analysis, the percentage of putative miR-17 seed family targets showed a gradual increase from the HL miRNA-targetome to 'miR-17 targets' and was the highest in the 'potent miR-17 targets' (Figure 4A). Fifty percent of all gene transcripts in 'miR-17 targets' and 67% of all gene transcripts in 'potent miR-17 targets' contained at least one 6-mer matching site in the 3′-UTR (Figure 4A). When less stringent conditions (6-mer miR-17 seed matching site with GU wobble allowed) were applied and the search was expanded to include 5′-UTRs and coding sequences, 76% of 'miR-17 targets' and 82% of 'potent miR-17 targets' contained at least one miR-17 seed matching site in anywhere of the entire gene transcript (Figure 4B, Supplementary Data 1 and 5).

As a negative control seed matching sites for miR-220 were also analyzed (Figure 4C) and the percentages were normalized to the percentages found in the genome (Figure 4D). In this analysis, the enrichment of gene transcripts with miR-17 seed matching site in the 'potent miR-17 targets' reached up to 2-fold for 6-mer and up to 11-fold for 8-mer site while the enrichment of miR-220 seed matching site was consistently low (0–1.3-fold) in all three groups (Figure 4D).

Higher depletion folds appeared to be correlated with the number and density (average number of 6-mer sites/kb) of miR-17 seed matching sites in the 3′-UTR (Figure 5). The 'potent miR-17 targets' had the highest density for miR-17 seed matching site compared with 'miR-17 targets' and 'non-miR-17 targets' (Figure 5A). Enrichment of gene transcripts with multiple miR-17 seed matching sites in the 'potent miR-17 targets' reached up to 9-fold for 6-mer and 55-fold for 8-mer site (Figure 5B). These results indicated that our approach led to an increased number of gene transcripts with single and multiple miR-17 seed matching sites.

In L428 cells transfected with anti-miR-220, we did not observe a correlation of higher depletion fold with percentage of probes with miR-220 seed matching sites (both 6-mer and 8mer) (Supplementary Data 4). This indicated that no miR-220 targets are identified with this approach, which is consistent with the lack of miR-220 expression in the HL cells. To determine depletion of non-specific probes due to the transfection procedure, we compared anti-miR-220 depleted probes to anti-miR-17/20/93/106 depleted probes. In L428 cells, 154 probes were depleted in both anti-miR-17/20/93/106 and anti-miR-220 transfected cells (Supplementary Data 1). Sixty-two percent (96/154) of these consistently depleted probes contain at least one perfect 6-mer seed matching site for miR-17 in the 5′-UTR, coding region and/or 3′-UTR of the gene transcript while 39% of them (60/154) contain at least one perfect 6-mer seed matching site for both miR-17 and miR-220 in the 5′-UTR, coding region and/or 3′-UTR (Supplementary Data 1). Using less stringent conditions for miR-17 seed family target (i.e. 6-mer seed matching site with GU wobble allowed in 5′-UTR, coding region and 3′UTR), 73% (113/154) of these consistently depleted probes were identified as potential targets of

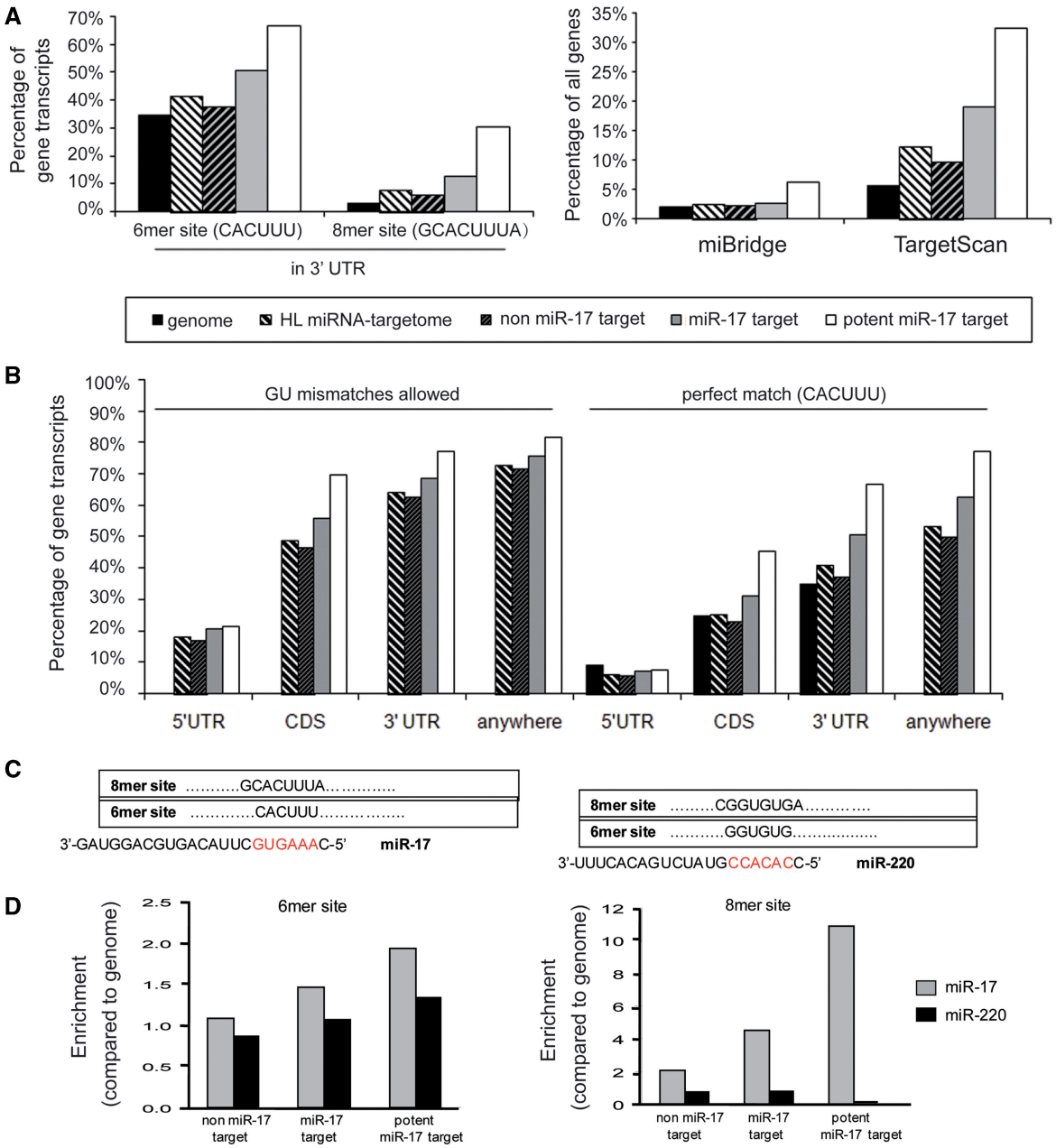

Figure 4. Enrichment of miR-17 seed family targets was correlated with higher depletion fold upon inhibition of the miR-17 seed family. (**A**) Percentage of miR-17 seed family targets by all definitions (presence of 6-mer site and 8-mer sites in 3′-UTRs, prediction by programs) was always highest in the 'potent miR-17 targets'. (**B**) Analysis of 6-mer miR-17 seed matching site with GU wobble allowed in the entire gene transcript revealed up to 76% of 'miR-17 targets' and 82% of 'potent miR-17 targets' with at least one miR-17 seed matching site in the entire gene transcript. (**C**) 6-mer and 8-mer seed matching sites for miR-17 and miR-220. (**D**) Enrichment of gene transcripts with miR-17 seed matching sites is correlated with higher depletion fold upon inhibition of the miR-17 seed family. In contrast, enrichment of miR-220 seed matching site, a miRNA which is not expressed in L428 is minimal.

miR-17 seed family. Based on these data we did not exclude them from the 'miR-17 target' list.

Validation by luciferase reporter assay

To validate the results generated from this RIP-Chip approach, 13 genes, namely *ADRB2, CCL1, CD274, FBXO31, GPR137B, NPAT, OBFC2A, RAB12, RBJ, SGK1, YES1, ZNF22* and *ZNFX1* (Figure 6), were chosen for luciferase reporter assay. These genes can be further categorized into groups according to their depletion fold in the Ago2-IP fraction upon miR-17/20/93/106 inhibition ('non-miR-17 targets', 'miR-17 targets' or 'potent miR-17 targets'), presence of 6-mer and 8-mer site for miR-17 in their 3′-UTRs (Table 2).

ADRB2 and *SGK1* were 'non-miR-17 targets' according to the RIP-Chip experiment and contained no 6-mer site for miR-17 in the 3′-UTRs. These two genes were negative

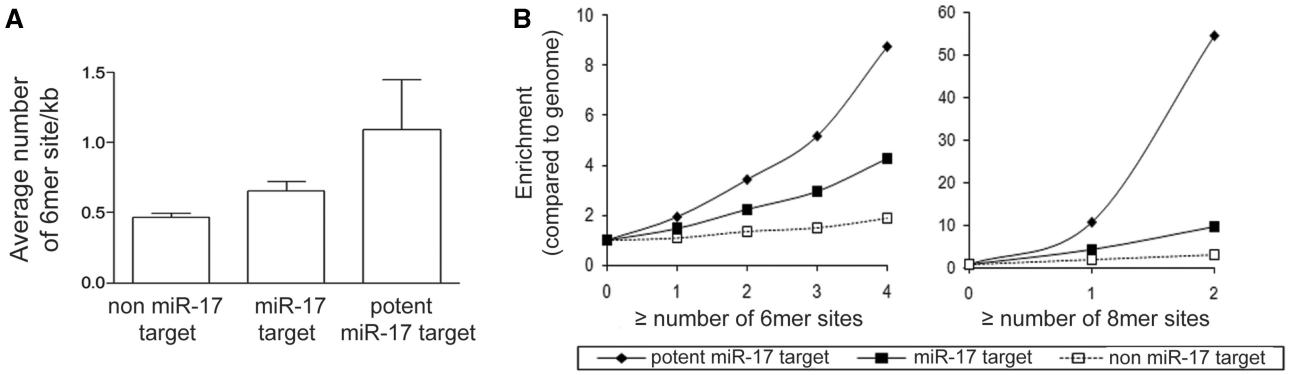

Figure 5. Gene transcripts with higher depletion fold upon inhibition of the miR-17 seed family had higher density and number of miR-17 seed matching sites in the 3′-UTRs. (**A**) 'Potent miR-17 targets' had the highest density of miR-17 seed matching sites in the 3′-UTRs. Mean with 95% confidence interval is shown. The data is statistically significant, with $P<0.0001$ (one-way ANOVA). (**B**) Enrichment of gene transcripts with multiple miR-17 seed matching sites was correlated with higher depletion fold upon inhibition of the miR-17 seed family.

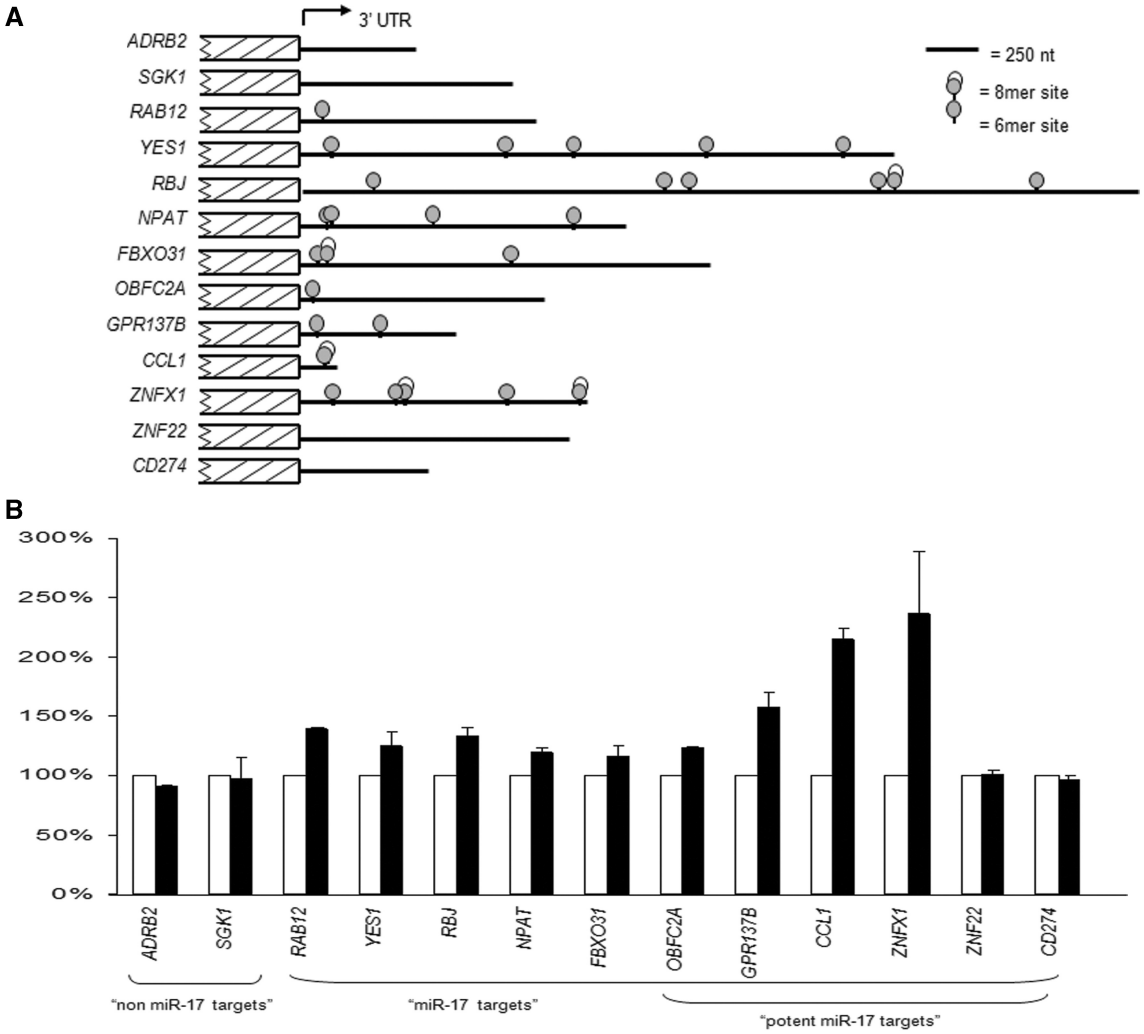

Figure 6. Validation of targets of the miR-17 seed family by luciferase reporter assay. (**A**) Schematic diagram of the genes cloned into psiCHECK2 vector for luciferase reporter assay. Potential miR-17/20/93/106 binding sites (6-mer and 8-mer sites) are indicated. (**B**) Luciferase reporter assay for the selected genes confirmed *RAB12, YES1, RBJ, NPAT, FBXO31, OBFC2A, GPR137B, CCL1* and *ZNFX1* as targets of the miR-17 seed family. Open bar, transfection with construct only. Filled bar, construct co-transfected with anti-miR-17/20/93/106.

Table 2. Genes selected for luciferase reporter assay

		Depletion fold	miR-17 site in 3'-UTR		Confirmed by luciferase reporter assay
			6-mer	8-mer	
non miR-17 targets					
ADRB2	NM 000024	1.37	0	0	N
SGK1	NM 005627	1.44	0	0	N
RAB12	NM 001025300	1.73	1	0	Y
miR-17 targets					
YES1	NM 005433	2.08	5	0	Y
RBJ	NM 016544	2.53	6	1	Y
NPAT	NM 002519	3.54	4	0	Y
FBX031	NM 024735	3.78	3	1	Y
OBFC2A[a]	NM 001031716	4.64	1	0	Y
GPR137B[a]	NM 003272	4.88	2	0	Y
CCL1[a]	NM 002981	5.67	1	1	Y
ZNFX1[a]	NM 021035	9.97	5	2	Y
ZNF22[a]	NM 006963	5.14	0	0	N
CD274[a]	ENST0000038157	5.23	0	0	N

[a]Also belong to the 'potent miR-17 targets'.

in the luciferase reporter assay (Figure 6). *RAB12* was marginally depleted in RIP-Chip (1.73-fold) and was listed as a 'non-miR-17 target'. In contrast to *ADRB2* and *SGK1*, *RAB12* contained a 6-mer site for miR-17 and showed enhanced luciferase activities upon inhibition of the miR-17 seed family (Figure 6). All 'miR-17 targets' and 'potent miR-17 targets' identified from the RIP-Chip experiment that contained at least one 6-mer site for miR-17 in the 3′-UTRs (*CCL1, FBXO31, GPR137B, NPAT, OBFC2A, RBJ, YES1* and *ZNFX1*) showed increased luciferase signals upon inhibition of the miR-17 seed family (Figure 6). A more pronounced increase was observed with the 'potent miR-17 targets' that contained at least one 6-mer site for miR-17. The two 'potent miR-17 targets' without a 6-mer site for miR-17 in the 3′-UTR (*CD274* and *ZNF22*) did not yield increased signals in the luciferase reporter assays upon inhibition of the miR-17 seed family (Figure 6). Notably, five of the nine genes showing enhanced luciferase signals have at least one 6-mer but not a 8-mer site for miR-17 in the 3′-UTRs (Table 2).

DISCUSSION

We have demonstrated the effectiveness of a high throughput method for identification of endogenous miRNA targets in untreated human cells. This approach not only allows the analysis of the complete transcriptome for miRNA targets but also permits a more direct identification of physiologically relevant miRNA targets in human cells and tissues. Subsequently, in combination with anti-miRNA strategy the RIP-Chip approach led to high throughput identification of endogenous targets of the miR-17 seed family.

Prediction programs for miRNA targets often predict all possible targets irrespective of their physiologically relevance and their co-expression with the corresponding miRNA. Consequently, the false positive rate for prediction programs can be high and selection of the most relevant genes from a long list of predicted miRNA targets is difficult. Up to date there are several publications showing the feasibility of the biochemical RISC-IP approach to identify miRNA targets. The experiments described in these publications were performed in *Drosophila melanogaster* (15), by IP of AIN-1 and AIN-2, other RISC associated proteins in *Caenorhabditis elegans* (16), using cloning based strategy in the human embryonic kidney HEK293 cell line (17) and tagged Ago proteins also in the HEK293 cell line (18–20). In the latter studies, experiments were performed using tagged Ago proteins and miRNAs that are not endogenously expressed in HEK293 for miRNA target identification. This may result in targets that normally are not co-expressed with their targeting miRNA and hence the physiological relevance is questionable. The approach we demonstrated here identifies mRNAs which are associated with endogenous miRNA in wild-type human Ago2 containing complex and thus allows direct screening of any human tissue or cell type. Also, we showed that cross-analysis of the results from an anti-miRNA strategy combined with RIP-Chip and presence of a 6-mer site in the 3′-UTR, irrespective of program prediction, can be sufficient to confirm specific miRNA targeting.

Table 3. Known miRNA target genes that have been found in the miRNA-targetome

miRNA	Target
let-7/miR-98	*KRAS, CASP3*
miR-15/16	*DMTF1, CCND1, CCNE1*
miR-17/20/93/106	*NCOA3*[a], *RB1*[a], *TGFBR2*[a], *E2F3, ARID4B*[a], *MYLIP, CDKN1A, TP53INP1*[a]
miR-21	*TPM1*
miR-29	*MCL1*

[a]Proven miR-17 targets which were also revealed in the RIP-Chip approach with inhibition of the miR-17 seed family.

Fifteen known targets of the top 5% expressed miRNAs (13,22,26–36) were identified in our HL miRNA-targetome (Table 3), showing the effectiveness of our approach. Within the HL miRNA-targetome we found a significant enrichment of genes that are associated with the p53 signaling pathway, ubiquitin mediated proteolysis, apoptosis and regulation of cell size (data not shown), features which are related to the nature of the tumor cells of HL. This HL miRNA-targetome includes genes which are known to be inactivated by mutations in HL cases, like *FAS, NFKB1A, NFKB1E, SOCS1* and *TNFAIP3* (37–42). These results reflect the physiological relevance of our study.

Combining anti-miRNA strategy with RIP-Chip revealed 1189 gene transcripts ('miR-17 target') that were ≥2-fold depleted from the Ago2-IP upon miR-17/20/93/106 inhibition. Comparison of these 1189 'miR-17 targets' to the 990 miR-17 target genes predicted by TargetScan (release 5.0) revealed an overlap of ∼20%. The limited overlap may be due to the inclusion of all genes with conserved target sites in 3′-UTR by the

TargetScan prediction program whereas in our experimental approach, we evaluated only endogenous transcripts. According to the results from the luciferase reporter assay, all genes with $\geq$2 depletion fold and presence of the 6-mer site for miR-17 in the 3′-UTR can be directly considered as targets of the miR-17 seed family. This resulted in 599 gene transcripts that were identified as miR-17 targets in our approach. However, the remaining 590 gene transcripts included in the 'miR-17 targets' list lacked 6-mer sites in the 3′-UTRs, like *ZNF22* and *CD274*. It might be speculated that the target sites for these genes are present in the coding region and/or the 5′-UTRs, as has been reported for p16 regulation by miR-24 (43) and *SEC24D* regulation by miR-605 (25). To address this question, we re-analyzed the entire miRNA-targetome of HL for presence of miR-17 binding site with the less stringent conditions i.e. 6-mer miR-17 seed matching site with GU wobble allowed. Moreover, we expanded the seed matching search into 5′-UTRs and coding regions (Figure 4B, Supplementary Data 1 and 5). In L428, up to 88% of all 'potent miR-17 targets' (including *ZNF22* and *CD274*) and 76% of 'miR-17 targets' contained at least one 6-mer miR-17 seed-matching site (Supplementary Data 1 and 5). This result is in line with the expectation that miRNA targets should contain target sites matching to the seed sequence of miRNA. In our opinion, the percentage did not reach 100% because the analysis was made with the assumption that only site matching to the 5′ seed of the miRNA is important for targeting and sequence complementarity between the 3′ end of the miRNA to the target is ignored. We cannot exclude presence of genes in the miRNA-targetome due to non-specific binding. Also, we cannot exclude the possibility of newly acquired or lost of miR-17 seed family target sites in gene transcripts that were expressed in the HL cell models. These two issues can be addressed by application of the recently published technique called high throughput sequencing of RNA isolated by crosslinking IP (HITS-CLIP) (44,45). In HITS-CLIP, the extra crosslinking step induced a covalent binding of the RNA to RISC, allowing a more stringent purification. Also, the exact miRNA binding sites can be identified by deep sequencing.

In the HL miRNA-targetome, co-regulation of a gene transcript by multiple miRNAs is common (as indicated in our *in silico* analysis, Supplementary Data 1). In the RIP-Chip experiment with inhibition of the miR-17 seed family, we identified five out of eight of the miR-17 targets, *NCOA3, RB1, TGFBR2, ARID4B, TP53INP1* that were experimentally proven elsewhere (26,30–32). The other three experimentally proven miR-17 targets (*E2F3, MYLIP* and *CDKN1A*) (22,28,32) had depletion fold of 1–1.8 and hence were categorized in the 'non-miR-17 targets'. Similarly, we validated *RAB12* as a target of the miR-17 seed family, but it was only 1.73-fold depleted upon inhibition of the miR-17 seed family. It can be speculated that inhibition of the miR-17 seed family alone is insufficient to remove *RAB12, E2F3, MYLIP* and *CDKN1A* from the Ago2-IP fraction, based on the presence of predicted target sites for let-7, miR-15, miR-25, miR-19 and miR-29 in the 3′-UTR of these genes. Although we cannot exclude the presence of miR-17 seed family targets in the 'non-miR-17 targets' group, these genes most likely are simultaneously targeted by miRNAs other than the miR-17 seed family and hence minimal effects are seen upon inhibition of only miR-17/20/93/106. The complexity of miRNA:mRNA interaction (46) still awaits to be addressed.

Consistent with the observation from the Bartel group who used a proteomics approach to identify miRNA targets (14), we found a higher enrichment of 8-mer sites as compared with 6-mer sites in the RIP-Chip identified miRNA targets. However, five out of nine targets of the miR-17 seed family verified in our luciferase reporter assay have 6-mer but not 8-mer site in the 3′-UTRs. Our results suggest that presence of the 8-mer site in the 3′-UTR is a good indicator to identify miRNA-specific targets, but presence of the 8-mer site is not obligatory for effective targeting by miRNA. Recently, the Ambros group analyzed mRNA transcripts which were identified by IP of AIN proteins in *C. elegans* and created a program called mirWIP (47). This program considers various features of the experimentally identified miRNA targets (like structural accessibility of target sequences, total free energy of miRNA-target binding) and hence a better refinement of the miRNA prediction algorithm can be achieved. Within the scope of our study, perfect 6-mer seed matching sites in the 3′-UTR is still the best criterion to identify miR-17 seed family targets from the genome, as this criterion clearly discriminate the two groups better than other criteria (Figure 4B, Supplementary Data 5). Despite the higher coverage observed for the analysis which allowed GU mismatches, these criteria suffer from a high background precluding an effective analysis for enrichment of miRNA targets (Figure 4B, Supplementary Data 5). Hence, it will be interesting to include the human miRNA targets identified in our study for mirWIP analysis and sort out the conditions which discriminate between the 'miR-17 targets' and background.

In conclusion, we have established a high throughput approach to identify endogenous miRNA targets of untreated human cells and provide an option to evaluate miRNA seed family specific targets. This is an important improvement as current methods lack the advantage of high throughput and unbiased identification of physiologically relevant target genes.

SUPPLEMENTARY DATA

Supplementary Data are available at NAR Online.

ACKNOWLEDGEMENTS

The authors thank George Bell from Bioinformatics and Research Computing, Whitehead Institute, for information about the TargetScan 3′-UTR database and Inhan Lee from Center for Computational Medicine and Biology, University of Michigan for information about the miBridge database.

FUNDING

Ubbo Emmius Foundation, University Medical Center Groningen [to L.P.T.]; the Dutch Cancer Society [2006-3643 to A.v.d.B.] and the Netherlands Organization for Scientific Research [NWO VIDI 971-36-400 to O.C.M.S.]. Funding for open access charge: Department of Pathology, University Medical Center Groningen.

Conflict of interest statement. None declared.

REFERENCES

1. Lee,R.C., Feinbaum,R.L. and Ambros,V. (1993) The C. elegans heterochronic gene lin-4 encodes small RNAs with antisense complementarity to lin-14. *Cell*, **75**, 843–854.
2. Bartel,D.P. (2004) MicroRNAs: genomics, biogenesis, mechanism, and function. *Cell*, **116**, 281–297.
3. Ambros,V. (2004) The functions of animal microRNAs. *Nature*, **431**, 350–355.
4. Liang,Y., Ridzon,D., Wong,L. and Chen,C. (2007) Characterization of microRNA expression profiles in normal human tissues. *BMC. Genomics*, **8**, 166.
5. Ramkissoon,S.H., Mainwaring,L.A., Ogasawara,Y., Keyvanfar,K., McCoy,J.P. Jr, Sloand,E.M., Kajigaya,S. and Young,N.S. (2006) Hematopoietic-specific microRNA expression in human cells. *Leuk. Res.*, **30**, 643–647.
6. Georgantas,R.W. III, Hildreth,R., Morisot,S., Alder,J., Liu,C.G., Heimfeld,S., Calin,G.A., Croce,C.M. and Civin,C.I. (2007) CD34+ hematopoietic stem-progenitor cell microRNA expression and function: a circuit diagram of differentiation control. *Proc. Natl Acad. Sci. USA*, **104**, 2750–2755.
7. Chen,C.Z., Li,L., Lodish,H.F. and Bartel,D.P. (2004) MicroRNAs modulate hematopoietic lineage differentiation. *Science*, **303**, 83–86.
8. John,B., Enright,A.J., Aravin,A., Tuschl,T., Sander,C. and Marks,D.S. (2004) Human MicroRNA targets. *PLoS Biol.*, **2**, e363.
9. Lewis,B.P., Shih,I.H., Jones-Rhoades,M.W., Bartel,D.P. and Burge,C.B. (2003) Prediction of mammalian microRNA targets. *Cell*, **115**, 787–798.
10. Griffiths-Jones,S., Saini,H.K., van,D.S. and Enright,A.J. (2008) miRBase: tools for microRNA genomics. *Nucleic Acids Res.*, **36**, D154–D158.
11. Lewis,B.P., Burge,C.B. and Bartel,D.P. (2005) Conserved seed pairing, often flanked by adenosines, indicates that thousands of human genes are microRNA targets. *Cell*, **120**, 15–20.
12. Sethupathy,P., Megraw,M. and Hatzigeorgiou,A.G. (2006) A guide through present computational approaches for the identification of mammalian microRNA targets. *Nat. Meth.*, **3**, 881–886.
13. Zhu,S., Si,M.L., Wu,H. and Mo,Y.Y. (2007) MicroRNA-21 targets the tumor suppressor gene tropomyosin 1 (TPM1). *J. Biol. Chem.*, **282**, 14328–14336.
14. Baek,D., Villen,J., Shin,C., Camargo,F.D., Gygi,S.P. and Bartel,D.P. (2008) The impact of microRNAs on protein output. *Nature*, **455**, 64–71.
15. Easow,G., Teleman,A.A. and Cohen,S.M. (2007) Isolation of microRNA targets by miRNP immunopurification. *RNA*, **13**, 1198–1204.
16. Zhang,L., Ding,L., Cheung,T.H., Dong,M.Q., Chen,J., Sewell,A.K., Liu,X., Yates,J.R. III and Han,M. (2007) Systematic identification of C. elegans miRISC proteins, miRNAs, and mRNA targets by their interactions with GW182 proteins AIN-1 and AIN-2. *Mol. Cell*, **28**, 598–613.
17. Beitzinger,M., Peters,L., Zhu,J.Y., Kremmer,E. and Meister,G. (2007) Identification of human microRNA targets from isolated argonaute protein complexes. *RNA. Biol.*, **4**, 76–84.
18. Karginov,F.V., Conaco,C., Xuan,Z., Schmidt,B.H., Parker,J.S., Mandel,G. and Hannon,G.J. (2007) A biochemical approach to identifying microRNA targets. *Proc. Natl Acad. Sci. USA*, **104**, 19291–19296.
19. Hendrickson,D.G., Hogan,D.J., Herschlag,D., Ferrell,J.E. and Brown,P.O. (2008) Systematic identification of mRNAs recruited to argonaute 2 by specific microRNAs and corresponding changes in transcript abundance. *PLoS. ONE*, **3**, e2126.
20. Landthaler,M., Gaidatzis,D., Rothballer,A., Chen,P.Y., Soll,S.J., Dinic,L., Ojo,T., Hafner,M., Zavolan,M. and Tuschl,T. (2008) Molecular characterization of human Argonaute-containing ribonucleoprotein complexes and their bound target mRNAs. *RNA*, **14**, 2580–2596.
21. Gibcus,J.H., Tan,L.P., Harms,G., Schakel,R.N., de Jong,D., Blokzijl,T., Moller,P., Poppema,S., Kroesen,B.J. and van den Berg,A. (2009) Hodgkin lymphoma cell lines are characterized by a specific miRNA expression profile. *Neoplasia.*, **11**, 167–176.
22. Ivanovska,I., Ball,A.S., Diaz,R.L., Magnus,J.F., Kibukawa,M., Schelter,J.M., Kobayashi,S.V., Lim,L., Burchard,J., Jackson,A.L. *et al.* (2008) MicroRNAs in the miR-106b family regulate p21/CDKN1A and promote cell cycle progression. *Mol. Cell Biol.*, **28**, 2167–2174.
23. Keene,J.D., Komisarow,J.M. and Friedersdorf,M.B. (2006) RIP-Chip: the isolation and identification of mRNAs, microRNAs and protein components of ribonucleoprotein complexes from cell extracts. *Nat. Protoc.*, **1**, 302–307.
24. Edgar,R., Domrachev,M. and Lash,A.E. (2002) Gene Expression Omnibus: NCBI gene expression and hybridization array data repository. *Nucleic Acids Res.*, **30**, 207–210.
25. Lee,I., Ajay,S.S., Yook,J.I., Kim,H.S., Hong,S.H., Kim,N.H., Dhanasekaran,S.M., Chinnaiyan,A. and Athey,B.D. (2009) New class of microRNA targets containing simultaneous 5′-UTR and 3′-UTR interaction sites. *Genome Res.*, **19**, 1175–1183.
26. Hossain,A., Kuo,M.T. and Saunders,G.F. (2006) Mir-17-5p regulates breast cancer cell proliferation by inhibiting translation of AIB1 mRNA. *Mol. Cell Biol.*, **26**, 8191–8201.
27. Kiriakidou,M., Nelson,P.T., Kouranov,A., Fitziev,P., Bouyioukos,C., Mourelatos,Z. and Hatzigeorgiou,A. (2004) A combined computational-experimental approach predicts human microRNA targets. *Genes Dev.*, **18**, 1165–1178.
28. Sylvestre,Y., De Guire,V., Querido,E., Mukhopadhyay,U.K., Bourdeau,V., Major,F., Ferbeyre,G. and Chartrand,P. (2007) An E2F/miR-20a autoregulatory feedback loop. *J. Biol. Chem.*, **282**, 2135–2143.
29. Liu,Q., Fu,H., Sun,F., Zhang,H., Tie,Y., Zhu,J., Xing,R., Sun,Z. and Zheng,X. (2008) miR-16 family induces cell cycle arrest by regulating multiple cell cycle genes. *Nucleic Acids Res.*, **36**, 5391–5404.
30. Yeung,M.L., Yasunaga,J., Bennasser,Y., Dusetti,N., Harris,D., Ahmad,N., Matsuoka,M. and Jeang,K.T. (2008) Roles for microRNAs, miR-93 and miR-130b, and tumor protein 53-induced nuclear protein 1 tumor suppressor in cell growth dysregulation by human T-cell lymphotrophic virus 1. *Cancer Res.*, **68**, 8976–8985.
31. Volinia,S., Calin,G.A., Liu,C.G., Ambs,S., Cimmino,A., Petrocca,F., Visone,R., Iorio,M., Roldo,C., Ferracin,M. *et al.* (2006) A microRNA expression signature of human solid tumors defines cancer gene targets. *Proc. Natl Acad. Sci. USA*, **103**, 2257–2261.
32. Landais,S., Landry,S., Legault,P. and Rassart,E. (2007) Oncogenic potential of the miR-106-363 cluster and its implication in human T-cell leukemia. *Cancer Res.*, **67**, 5699–5707.
33. Johnson,S.M., Grosshans,H., Shingara,J., Byrom,M., Jarvis,R., Cheng,A., Labourier,E., Reinert,K.L., Brown,D. and Slack,F.J. (2005) RAS is regulated by the let-7 microRNA family. *Cell*, **120**, 635–647.
34. Tsang,W.P. and Kwok,T.T. (2008) Let-7a microRNA suppresses therapeutics-induced cancer cell death by targeting caspase-3. *Apoptosis*, **13**, 1215–1222.
35. Bonci,D., Coppola,V., Musumeci,M., Addario,A., Giuffrida,R., Memeo,L., D'Urso,L., Pagliuca,A., Biffoni,M., Labbaye,C. *et al.* (2008) The miR-15a-miR-16-1 cluster controls prostate cancer by targeting multiple oncogenic activities. *Nat. Med.*, **14**, 1271–1277.
36. Mott,J.L., Kobayashi,S., Bronk,S.F. and Gores,G.J. (2007) mir-29 regulates Mcl-1 protein expression and apoptosis. *Oncogene*, **26**, 6133–6140.
37. Emmerich,F., Meiser,M., Hummel,M., Demel,G., Foss,H.D., Jundt,F., Mathas,S., Krappmann,D., Scheidereit,C., Stein,H. *et al.* (1999) Overexpression of I kappa B alpha without inhibition of

NF-kappaB activity and mutations in the I kappa B alpha gene in Reed-Sternberg cells. *Blood*, **94**, 3129–3134.
38. Cabannes,E., Khan,G., Aillet,F., Jarrett,R.F. and Hay,R.T. (1999) Mutations in the IkBa gene in Hodgkin's disease suggest a tumour suppressor role for IkappaBalpha. *Oncogene*, **18**, 3063–3070.
39. Emmerich,F., Theurich,S., Hummel,M., Haeffker,A., Vry,M.S., Dohner,K., Bommert,K., Stein,H. and Dorken,B. (2003) Inactivating I kappa B epsilon mutations in Hodgkin/Reed-Sternberg cells. *J. Pathol.*, **201**, 413–420.
40. Weniger,M.A., Melzner,I., Menz,C.K., Wegener,S., Bucur,A.J., Dorsch,K., Mattfeldt,T., Barth,T.F. and Moller,P. (2006) Mutations of the tumor suppressor gene SOCS-1 in classical Hodgkin lymphoma are frequent and associated with nuclear phospho-STAT5 accumulation. *Oncogene*, **25**, 2679–2684.
41. Schmitz,R., Hansmann,M.L., Bohle,V., Martin-Subero,J.I., Hartmann,S., Mechtersheimer,G., Klapper,W., Vater,I., Giefing,M., Gesk,S. *et al.* (2009) TNFAIP3 (A20) is a tumor suppressor gene in Hodgkin lymphoma and primary mediastinal B cell lymphoma. *J. Exp. Med.*, **206**, 981–989.
42. Maggio,E.M., van den Berg,A., de Jong,D., Diepstra,A. and Poppema,S. (2003) Low frequency of FAS mutations in Reed-Sternberg cells of Hodgkin's lymphoma. *Am. J. Pathol.*, **162**, 29–35.
43. Lal,A., Kim,H.H., Abdelmohsen,K., Kuwano,Y., Pullmann,R. Jr, Srikantan,S., Subrahmanyam,R., Martindale,J.L., Yang,X., Ahmed,F. *et al.* (2008) p16(INK4a) translation suppressed by miR-24. *PLoS ONE*, **3**, e1864.
44. Licatalosi,D.D., Mele,A., Fak,J.J., Ule,J., Kayikci,M., Chi,S.W., Clark,T.A., Schweitzer,A.C., Blume,J.E., Wang,X. *et al.* (2008) HITS-CLIP yields genome-wide insights into brain alternative RNA processing. *Nature*, **456**, 464–469.
45. Chi,S.W., Zang,J.B., Mele,A. and Darnell,R.B. (2009) Argonaute HITS-CLIP decodes microRNA-mRNA interaction maps. *Nature*, **460**, 479–486.
46. Rigoutsos,I. (2009) New tricks for animal microRNAs: targeting of amino acid coding regions at conserved and nonconserved sites. *Cancer Res.*, **69**, 3245–3248.
47. Hammell,M., Long,D., Zhang,L., Lee,A., Carmack,C.S., Han,M., Ding,Y. and Ambros,V. (2008) mirWIP: microRNA target prediction based on microRNA-containing ribonucleoprotein-enriched transcripts. *Nat. Methods*, **5**, 813–819.